PhD Second-Year Checkpoint
Updated Work Plan

Full Name	Bruno Rodrigues Pacheco e Murta
Institution	Universidade do Minho
Doctoral Programme	MAP-fis
Title of Dissertation	Quantum Many-Body Ground States via Digital Quantum Simulation
Supervisor	Prof. Joaquín Fernández-Rossier (INL)
Co-Supervisor	Prof. Nuno M. R. Peres (U. Minho)

Introduction

The PhD project carried out by Bruno Murta concerns the development of schemes to prepare quantum many-body states on digital quantum computers, particularly to determine the exact ground state of systems of correlated electrons, on the one hand, and of frustrated spins, on the other, within the context of condensed matter physics. Thus far, in the former case, Mr. Murta devised a routine [1] to initialize the Gutzwiller wave function [2], while in the latter Mr. Murta explored the implementation [3] of Valence Bond States [4] on quantum hardware. The updated work plan for the upcoming year will follow a similar twofold approach, comprising a research line on frustrated quantum spin systems and another on strongly-correlated electrons.

The research project on quantum spin models will involve the application of the variational quantum eigensolver (VQE) [5]. The first task will correspond to exploring how to simulate quantum spin-1 (and, more generally, higher-spin) models on a quantum computer via VQE. This is a natural follow-up project of the initialization of Valence Bond States on quantum hardware. In addition, VQE methods to tackle quantum spin-$\frac{1}{2}$ models will also be considered. In particular, a parameterized ansatz [6] inspired by the Resonating Valence Bond (RVB) states [7] will be considered. Mr. Murta will benchmark this ansatz for the spin-$\frac{1}{2}$ Heisenberg model and seek potential improvements of its structure.

The main goal of the project on correlated electrons will be to bypass the repetition overhead in the implementation of the Gutzwiller operator [2] on quantum computers. Two strategies will be considered: first, applying the Gutzwiller operator as a post-processing step, thus avoiding its explicit execution on quantum hardware; second, finding a unitary transformation that maps the initial state to the normalized Gutzwiller wave function akin to the quantum imaginary-time evolution (QITE) method [8]. The use of the Gutzwiller wave function as the input state for the simulation of the Fermi-Hubbard model with VQE will also be benchmarked.

Regarding the learning outcomes for the forthcoming year, the main one will be the exploration of VQE methods [5] to study quantum lattice models. Another valuable skill to be developed will be the simulation of higher-spin (particularly spin-1) models in conventional and quantum hardware [8]. Mr. Murta will also continue to study tensor network methods [9, 10] as part of a study group.

The next section provides a more detailed view of the two upcoming research projects, briefly introducing the relevant background and listing some open questions and potential lines of research.

Upcoming Research Projects: A Preliminary View

Quantum Spin Systems: Higher Spins and Resonating Valence Bond States

The motivation for the preparation of Valence Bond States (VBS) [4] on quantum hardware is to use them as the starting point of a digital quantum simulation algorithm that aims to find low-lying excited states of the corresponding AKLT model or the ground states of nearby but non-integrable models. With the noisy intermediate-scale quantum computers currently at our disposal, the natural approach is to use hybrid variational algorithms such as VQE [5]. However, although VQE has been employed to simulate quantum spin-$\frac{1}{2}$ models [11, 12, 13, 14, 15, 16], its application to spin-1 and higher-spin models remains largely unexplored.

As a proof of concept of the application envisioned for VBS on quantum hardware, a VQE simulation of the one-dimensional bilinear-biquadratic spin-1 Hamiltonian

$$\mathcal{H}^{S=1}_{\mathrm{BLBQ}}(\beta) = \sum_{n=1}^{N} \vec{S}_n \cdot \vec{S}_{n+1} + \beta(\vec{S}_n \cdot \vec{S}_{n+1})^2 \tag{1}$$

will be explored. Specifically, the starting point will be the spin-1 VBS, which is the exact and unique[1] ground state of $H^{S=1}_{\mathrm{BLBQ}}$ at $\beta = \frac{1}{3}$. The parameter β will then be reduced towards 0, at which point the spin-1 Heisenberg model is attained. The main goal will be to compute the ground state away from the integrable point $\beta = \frac{1}{3}$. The gap may also be computed by finding the lowest-lying excited state. The simplest way to accomplish this is to add an extra term to the Hamiltonian, $E\,|\phi_0^{\mathrm{estimate}}\rangle\,\langle\phi_0^{\mathrm{estimate}}|$, with a large energy penalty E, thus ensuring that our search space is orthogonal to the previously obtained ground state $|\phi_0^{\mathrm{estimate}}\rangle$ [17, 18].

The simulation of quantum spin-1 models on a digital quantum computer demands a few changes relative to the standard case of spins-$\frac{1}{2}$. The first corresponds to the encoding of a spin-1 in terms of qubits. Since there are $2 \times 1 + 1 = 3$ basis states, a minimum of two qubits per spin-1 are required, resulting in a fourth redundant basis state. The natural option is to follow the mapping

$$|S=1, S_z=1\rangle \leftrightarrow |00\rangle\,,\ |S=1, S_z=0\rangle \leftrightarrow \frac{|01\rangle + |10\rangle}{\sqrt{2}},\ |S=1, S_z=-1\rangle \leftrightarrow |11\rangle\,,$$

as in the construction of the VBS. In the original 3-dimensional local Hilbert space, the matrix representations of the local spin operators $\hat{S}^x$, $\hat{S}^y$ and $\hat{S}^z$ space take the form

$$S^x = \frac{1}{\sqrt{2}}\begin{pmatrix} 0 & 1 & 0 \\ 1 & 0 & 1 \\ 0 & 1 & 0 \end{pmatrix},\ S^y = \frac{1}{\sqrt{2}i}\begin{pmatrix} 0 & 1 & 0 \\ -1 & 0 & 1 \\ 0 & -1 & 0 \end{pmatrix},\ S^z = \begin{pmatrix} 1 & 0 & 0 \\ 0 & 0 & 0 \\ 0 & 0 & -1 \end{pmatrix}, \tag{2}$$

while in the extended 4-dimensional Hilbert space we have

$$\mathbf{S}^x = \frac{1}{2}\begin{pmatrix} 0 & 1 & 1 & 0 \\ 1 & 0 & 0 & 1 \\ 1 & 0 & 0 & 1 \\ 0 & 1 & 1 & 0 \end{pmatrix},\ \mathbf{S}^y = \frac{1}{2i}\begin{pmatrix} 0 & 1 & 1 & 0 \\ -1 & 0 & 0 & 1 \\ -1 & 0 & 0 & 1 \\ 0 & -1 & -1 & 0 \end{pmatrix},\ \mathbf{S}^z = \begin{pmatrix} 1 & 0 & 0 & 0 \\ 0 & 0 & 0 & 0 \\ 0 & 0 & 0 & 0 \\ 0 & 0 & 0 & -1 \end{pmatrix}, \tag{3}$$

or, more compactly, $\mathbf{S}^\alpha = \sigma^\alpha \otimes \mathbb{1} + \mathbb{1} \otimes \sigma^\alpha$, where $\alpha = x, y, z$ and $\{\mathbb{1}, \sigma^x, \sigma^y, \sigma^z\}$ is the (spin-$\frac{1}{2}$) Pauli group. In summary, one just has to replace the spin-1 operators in the Hamiltonian shown in eq. 1 by their respective expressions in terms of spin-$\frac{1}{2}$ operators, which already gives rise to a sum of Pauli strings, the expectation values of which can be directly computed as usual.

[1] This uniqueness occurs only for periodic boundary conditions, otherwise there is a four-fold degeneracy.

The second change with respect to the spin-$\frac{1}{2}$ case corresponds to restricting the state to the physically relevant local 3-dimensional Hilbert space. In other words, the amplitude of the extra unphysical basis state $|S=0, S_z=0\rangle \equiv \frac{1}{\sqrt{2}}(|01\rangle - |10\rangle)$ must be set to zero at every site. There are three possible solutions to this problem.

The first solution replicates the overlap method mentioned above to compute low-lying excited states with VQE: an energy penalty $E\,|S=0, S_z=0\rangle\langle S=0, S_z=0|$ for every site is added to the cost function (i.e., to the Hamiltonian), thus preventing the parameterized ansatz from occupying the forbidden basis state. Note that this solution is possible because the input state, the VBS, is already confined to the physical spin-1 subspace.

The second solution allows the full extended Hilbert space to be explored throughout the optimization process, but at the end of the computation the obtained state is projected to the physical space as a classical post-processing step, which amounts to renormalizing the state, in a similar spirit to the computation of the expectation values of the GWF (cf. eq. (5)). This strategy is inspired by the theory of quantum optimal control, where faster high-fidelity operations are implemented by adding symmetry-breaking terms [19].

The third solution involves creating a parameterized circuit that only explores the physical subspace. This requires devising building blocks that do not mix the three physical basis states with the unphysical one at each site. For example, the analogue of a $R_y(\theta)$ gate for spin-1 could be

$$\begin{pmatrix} \cos(\theta/2) & 0 & 0 & -\sin(\theta/2) \\ 0 & 1 & 0 & 0 \\ 0 & 0 & 1 & 0 \\ \sin(\theta/2) & 0 & 0 & \cos(\theta/2) \end{pmatrix} \equiv$$

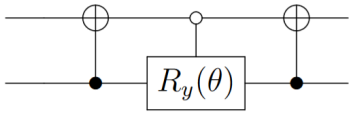

which creates linear superpositions of $|S=1, S_z=+1\rangle$ and $|S=1, S_z=-1\rangle$. Notice that, since there are three instead of two physical basis states, there are two other pairs of physical basis states that could be mixed. The challenge of this strategy is that single-qubit and two-qubit gates used as building blocks of parameterized circuits to simulate spins-$\frac{1}{2}$ are replaced by two-qubit and four-qubit gates for spins-1, which leads to a significantly greater depth per layer of the ansatz.

After considering the application of VQE to quantum spin-1 models, Mr. Murta will turn his attention to the more standard spin-$\frac{1}{2}$ case. Concretely, the RVB-inspired ansatz proposed by Seki *et al.* [6] will be considered. The starting point consists of the preparation of a product state of spin singlets at nearest-neighboring pairs, $\frac{1}{\sqrt{2}}(|\uparrow\downarrow\rangle - |\downarrow\uparrow\rangle)$. This state $|\Phi\rangle$ belongs to the subspace of $S=0$, in agreement with the exact ground state of the Heisenberg model on a bipartite lattice [20]. The parameterized circuit applied on top of this initial state (cf. Fig. 1(a)) repeats a single building block, the so-called exponential SWAP (eSWAP(θ)) gate:

$$e^{-i\mathrm{SWAP}\frac{\theta}{2}} = \begin{pmatrix} e^{-i\frac{\theta}{2}} & 0 & 0 & 0 \\ 0 & \cos(\frac{\theta}{2}) & -i\sin(\frac{\theta}{2}) & 0 \\ 0 & -i\sin(\frac{\theta}{2}) & \cos(\frac{\theta}{2}) & 0 \\ 0 & 0 & 0 & e^{-i\frac{\theta}{2}} \end{pmatrix} \equiv$$

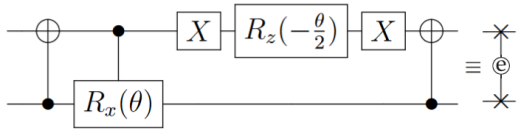

$\equiv$

The two-qubit circuit shown above is equivalent to the matrix up to a global phase factor of $e^{-i\theta/4}$. Importantly, this eSWAP gate preserves the spin SU(2) symmetry, which means the optimization is always restricted to the subspace of $S=0$.

A physical interpretation of the parameterized ansatz can be deduced by considering the effect of the eSWAP gate on a pair of spin singlets $|s_{ij}\rangle$ and $|s_{kl}\rangle$, where $|s_{ij}\rangle \equiv \frac{1}{\sqrt{2}}(|0\rangle_i |1\rangle_j - |1\rangle_i |0\rangle_j)$.

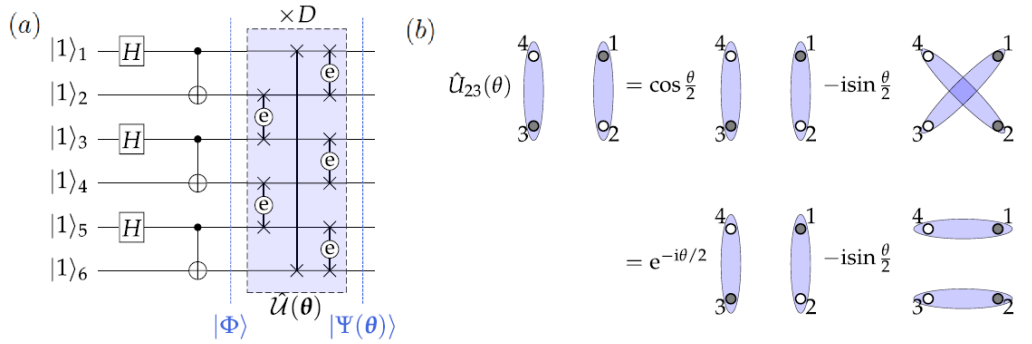

Figure 1: (a) RVB-inspired ansatz [6]. First layer prepares $|\Phi\rangle$, a product state of spin singlets $1/\sqrt{2}(|01\rangle - |10\rangle)$. Second layer corresponds to parameterized circuit, which amounts to repeating the same two-qubit operation, the eSWAP, at every pair of nearest-neighboring spins. This ansatz preserves the spin SU(2) symmetry, so the search space is restricted to the $S = 0$ subspace. (b) Action of eSWAP on a singlet-pair product state results in a superposition of two different singlet-pair product states. Last line explores the fact that any crossed diagram can be expressed in terms of non-crossed diagrams only [21, 22]. Figures adapted from [6].

Trivially, $\mathrm{SWAP}_{ij}\,|s_{ij}\rangle = |s_{ji}\rangle = -\,|s_{ij}\rangle$, therefore $\mathrm{SWAP}_{jk}\,|s_{ij}\rangle\,|s_{kl}\rangle = |s_{ik}\rangle\,|s_{jl}\rangle$, in which case

$$e\mathrm{SWAP}_{jk}(\theta)\,|s_{ij}\rangle\,|s_{kl}\rangle = \cos(\theta/2)\,|s_{ij}\rangle\,|s_{kl}\rangle - i\sin(\theta/2)\,|s_{ik}\rangle\,|s_{jl}\rangle\,. \tag{4}$$

In words, when acting on a singlet-pair product state, the eSWAP gate transforms it into a superposition of two different singlet-pair product states with parameterized amplitudes (cf. Fig. 1(b)). This ansatz therefore allows to construct a Resonating Valence Bond (RVB) state [7].

The starting point of this project involves the application of this RVB-inspired ansatz to the spin-$\frac{1}{2}$ Heisenberg model to predict how the number of layers required to attain a given fidelity threshold (relative to the exact ground state) scales with the system size. Another possibility is to apply this ansatz to probe the transition from the Majumdar-Ghosh model [23, 24] to the Heisenberg model, since the initial state $|\Phi\rangle$ (cf. Fig. 1(a)) is one of the two exact ground states of the former.

Correlated Electrons: Alternative Implementations of Gutzwiller Operator

The Gutzwiller wave function (GWF) is defined as $|\psi_G\rangle = \prod_{i=1}^{N} \hat{P}_G^{(i)}(g)\,|\psi_0\rangle$, where $\hat{P}_G^{(i)}(g) \equiv \mathbb{1} - g\hat{n}_{i,\uparrow}\hat{n}_{i,\downarrow}$ is the local Gutzwiller operator that reduces the amplitude of basis states with a doubly-occupied state $|\uparrow\downarrow\rangle$ at site i. If one wishes to use $|\psi_G\rangle$ as the starting point of a quantum algorithm, $\hat{P}_G^{(i)}(g)$ must be applied explicitly on quantum hardware. However, if one is merely interested in computing expectation values of the GWF (e.g., $\langle\psi_G|\hat{O}|\psi_G\rangle$ for some observable $\hat{O}$), $\hat{P}_G^{(i)}(g)$ can be executed as a post-processing step by noting that

$$\frac{\langle\psi_G|\hat{O}|\psi_G\rangle}{\langle\psi_G|\psi_G\rangle} = \frac{\langle\psi_0|\prod_{i=1}^{N}\hat{P}_G^{(i)}\hat{O}\prod_{i'=1}^{N}\hat{P}_G^{(i')}|\psi_0\rangle}{\langle\psi_0|\prod_{i=1}^{N}\hat{P}_G^{(i)}\prod_{i'=1}^{N}\hat{P}_G^{(i')}|\psi_0\rangle} \equiv \frac{\langle\psi_0|\hat{\tilde{O}}|\psi_0\rangle}{\langle\psi_0|\prod_{i=1}^{N}\hat{P}_G^{2(i)}|\psi_0\rangle}, \tag{5}$$

where $\hat{\tilde{O}} \equiv \prod_{i=1}^{N}\hat{P}_G^{(i)}\hat{O}\prod_{i'=1}^{N}\hat{P}_G^{(i')}$. Hence, one can determine the expectation value of an operator $\hat{O}$ with respect to the GWF by computing the expectation values of the projected operator $\hat{\tilde{O}}$ and of $\prod_{i=1}^{N}\hat{P}_G^{2(i)}$ relative to the noninteracting ground state $|\psi_0\rangle$ on quantum hardware.

In VQE, to compute the expectation value of the cost function (i.e., the Hamiltonian) to minimize the energy and find a good approximation to the exact ground state, and to compute expectation values of an observable with respect to the resulting approximation, one decomposes such an

Hermitian operator as a linear combination of strings of Pauli operators $\{\mathbb{1}, \sigma^x, \sigma^y, \sigma^z\}$. Since the Gutzwiller operator acts on each site separately, and given that each site is encoded by two qubits (due to spin), to find the transformed version of each Pauli string, $\tilde{S} \equiv \prod_{i=1}^{N} \hat{P}_G^{(i)} S \prod_{i'=1}^{N} \hat{P}_G^{(i')}$, it suffices to consider one site (i.e., two qubits) at a time. Suppose, e.g., that $S = \sigma^x_{i,\uparrow} \otimes \sigma^z_{i,\downarrow}$; the matrix representation of its transformed version, $\tilde{S} = \hat{P}_G^{\dagger(i)} S \hat{P}_G^{(i)}$, is

$$\begin{pmatrix} 1 & 0 & 0 & 0 \\ 0 & 1 & 0 & 0 \\ 0 & 0 & 1 & 0 \\ 0 & 0 & 0 & 1-g \end{pmatrix} \begin{pmatrix} 0 & 0 & 1 & 0 \\ 0 & 0 & 0 & -1 \\ 1 & 0 & 0 & 0 \\ 0 & -1 & 0 & 0 \end{pmatrix} \begin{pmatrix} 1 & 0 & 0 & 0 \\ 0 & 1 & 0 & 0 \\ 0 & 0 & 1 & 0 \\ 0 & 0 & 0 & 1-g \end{pmatrix} = \begin{pmatrix} 0 & 0 & 1 & 0 \\ 0 & 0 & 0 & g-1 \\ 1 & 0 & 0 & 0 \\ 0 & g-1 & 0 & 0 \end{pmatrix}.$$

This matrix can be diagonalized as $U\tilde{S}U^\dagger = D$, with $D = \mathrm{diag}(1, -1, 1-g, g-1)$ and

$$U = \frac{1}{\sqrt{2}} \begin{pmatrix} 1 & 0 & 1 & 0 \\ 1 & 0 & -1 & 0 \\ 0 & -1 & 0 & 1 \\ 0 & 1 & 0 & 1 \end{pmatrix} \equiv$$

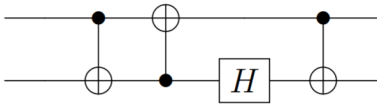

Hence, by applying the circuit shown above before the measurement of both qubits in the computational basis[2], the expectation value of $\tilde{S}$ is simply given by

$$\langle \tilde{S} \rangle = \frac{1 \cdot n_{00} + (-1) \cdot n_{01} + (1-g) n_{10} + (g-1) n_{11}}{n_{00} + n_{01} + n_{10} + n_{11}},$$

where n_{00} is the number of counts of the outcome 00. For any other Pauli string acting on site i, it is possible to find an equivalent two-qubit circuit, with depth of up to 3 CNOTs, that diagonalizes the transformed string. Hence, it is possible to compute expectation values of the GWF by just preparing the noninteracting ground state and adding an extra layer of at most 3 CNOTs.

Recently, Seki *et al.* [25] have explored this idea of estimating expectation values of the GWF without actually encoding it on quantum hardware. However, the Gutzwiller operator is expanded as a linear combination of unitaries via a discrete Hubbard-Stratonovich transformation [26], which leads to a sum over auxiliary Ising fields that is performed stochastically using the Monte Carlo method. The sampling weights are, in general, complex, and therefore the method suffers from the phase problem[3]. The approach herein discussed, in turn, does not face this issue.

More importantly, Mr. Murta and his supervisor, Prof. Fernández-Rossier, envision an adaptation of this method that goes beyond computing expectation values of the GWF. Specifically, instead of using the noninteracting ground state $|\psi_0\rangle$ as the state encoded in the quantum computer to calculate the expectation values of the transformed operators, one may instead use a previously optimized VQE ansatz, in a similar spirit to the method based on Jastrow operators proposed by Mazzola *et al.* [27]. Using the transformed Hamiltonian $\hat{\tilde{H}} \equiv \prod_{i=1}^{N} \hat{P}_G^{(i)} \hat{H} \prod_{i'=1}^{N} \hat{P}_G^{(i')}$ introduces an extra free parameter (the Gutzwiller parameter g), which can be tuned to further reduce the energy and improve upon the approximation to the exact ground state. Could this lead to a reduction of the depth and parameters of the ansatz required to attain a given accuracy with VQE?

Despite the convenience of forgoing the implementation of the Gutzwiller operator on a quantum computer, this post-processing strategy has the disadvantage of not allowing to use the GWF as the input state for VQE. Although one may, in principle, make use of the probabilistic method discussed in the summary report to initialize the GWF at the start of the simulation, for sufficiently large systems it would be convenient to develop a deterministic method to prepare the GWF.

[2] To compute the expectation value of the original operator, $S = \sigma^x_{i\uparrow} \otimes \sigma^z_{i\downarrow}$, one would just apply a Hadamard gate to the qubit that encodes the spin-$\uparrow$ orbital to transform to the x-basis before the measurement.

[3] The phase problem is a more severe variant of the sign problem in quantum Monte Carlo methods.

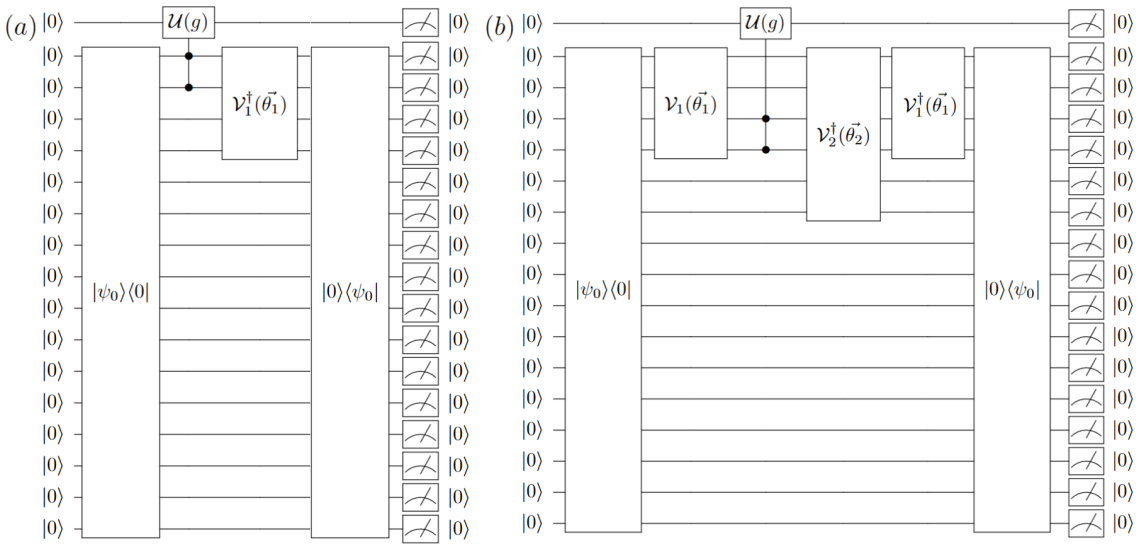

Figure 2: Scheme of implementation of Gutzwiller wave function via unitary operations. (a) First iteration. After preparing the noninteracting ground state $|\psi_0\rangle$ and applying the Gutzwiller operator at the first site, a parameterized ansatz $\mathcal{V}_1^\dagger(\vec{\theta_1})$ is tuned so as to invert the effect of the Gutzwiller operator. The optimal parameters are found by maximizing the overlap between the exact and approximate states, which is given by the probability of measuring all qubits in $|0\rangle$. (b) Second iteration. Now the reference state is $\mathcal{V}_1(\vec{\theta_1})\,|\psi_0\rangle$ instead of $|\psi_0\rangle$, and $\mathcal{V}_2^\dagger(\vec{\theta_2})$ is set to counter the effect of the Gutzwiller operator at the second site. The structure of the remaining iterations follows trivially. The number of qubits on which each $\mathcal{V}_i(\vec{\theta_i})$ acts should be as low as possible to simplify the optimization problem; such minimum width is to be determined empirically.

One possibility that will be explored to implement the Gutzwiller operator takes inspiration from the quantum imaginary-time evolution (QITE) method [8]. The idea is to find, one site at a time, a unitary $\mathcal{V}(\vec{\theta})$ that approximates the action of the local Gutzwiller operator (after normalization). The unitary $\mathcal{V}(\vec{\theta})$ is expressed in terms of a parameterized circuit with support on a set of qubits around the site in question (cf. Fig. 2(a)). For the first iteration, the optimal parameter values are found by maximizing the overlap with the exact outcome of the Gutzwiller operator acting on the noninteracting ground state, $|\,\langle\psi_0|\mathcal{V}_1^\dagger(\vec{\theta})\hat{P}_G^{(1)}|\psi_0\rangle\,|^2$. In the following iterations (cf. Fig. 2(b)), $|\psi_0\rangle$ is replaced by $\prod_i \mathcal{V}_i(\vec{\theta_i})\,|\psi_0\rangle$, where the product includes all previously found unitaries.

In order to present an advantage relative to just performing VQE from scratch with the noninteracting ground state, it is important that the width of the unitary transformations $\mathcal{V}_i(\vec{\theta_i})$ (i.e., the number of qubits of their support) is small, so that the resulting optimization problem is simple. This could be decisive for sufficiently large systems, where barren plateaus [28] can be difficult to overcome. Given the local nature of the Gutzwiller operator, is it possible to restrict the support of every $\mathcal{V}_i(\vec{\theta_i})$ to nearest-neighboring or next-nearest-neighboring sites of site i?

A final task of this project is to benchmark the use of the GWF as the initial state of VQE to tackle the Fermi-Hubbard model in one- and two-dimensional lattices of different sizes. Although using the GWF as the starting point requires an increase in the circuit depth relative to the initialization of the noninteracting or mean-field ground states, can this be compensated by significantly reducing the number of layers (and hence of parameters) of the parameterized ansatz?

References

[1] B. Murta and J. Fernández-Rossier *Phys. Rev. B*, vol. 103, p. L241113, 2021.

[2] M. C. Gutzwiller *Phys. Rev. Lett.*, vol. 10, pp. 159–162, 1963.

[3] B. Murta and J. Fernández-Rossier *In preparation.*

[4] I. Affleck, T. Kennedy, E. H. Lieb, and H. Tasaki *Phys. Rev. Lett.*, vol. 59, pp. 799–802, 1987.

[5] A. Peruzzo *et al. Nat. Commun.*, vol. 5, no. 1, p. 4213, 2014.

[6] K. Seki, T. Shirakawa, and S. Yunoki *Phys. Rev. A*, vol. 101, p. 052340, 2020.

[7] P. Anderson *Mater. Res. Bull.*, vol. 8, no. 2, pp. 153–160, 1973.

[8] M. Motta *et al. Nat. Phys.*, vol. 16, no. 2, pp. 205–210, 2020.

[9] R. Orús *Ann. Phys. (N. Y.)*, vol. 349, p. 117, 2014.

[10] J. von Delft, "Tensor networks 2020." `https://www2.physik.uni-muenchen.de/lehre/vorlesungen/sose_20/tensor_networks_20/`, last checked on February 10, 2022.

[11] J. Kattemölle and J. van Wezel *arXiv:2108.02175*, 2021.

[12] J. L. Bosse and A. Montanaro *arXiv:2108.08086*, 2021.

[13] A. C. Y. Li *et al. arXiv:2108.13375*, 2021.

[14] T. A. Bespalova and O. Kyriienko *arXiv:2109.13883*, 2021.

[15] A. T. Tan *et al. arXiv:2112.10333*, 2021.

[16] M. S. Jattana *et al. arXiv:2201.05065*, 2022.

[17] T. Jones *et al. Phys. Rev. A*, vol. 99, p. 062304, 2019.

[18] O. Higgott, D. Wang, and S. Brierley *Quantum*, vol. 3, p. 156, 2019.

[19] A. Choquette *et al. Phys. Rev. Research*, vol. 3, p. 023092, 2021.

[20] E. Lieb and D. Mattis *J. Math. Phys.*, vol. 3, no. 4, pp. 749–751, 1962.

[21] T. Oguchi and H. Kitatani *J. Phys. Soc. Jpn.*, vol. 58, no. 4, pp. 1403–1415, 1989.

[22] R. Saito *J. Phys. Soc. Jpn.*, vol. 59, no. 2, pp. 482–491, 1990.

[23] C. K. Majumdar and D. K. Ghosh *J. Math. Phys.*, vol. 10, no. 8, pp. 1399–1402, 1969.

[24] C. K. Majumdar *J. Phys. Condens. Matter*, vol. 3, no. 4, pp. 911–915, 1970.

[25] K. Seki, Y. Otsuka, and S. Yunoki *arXiv:2201.11381v1*, 2022.

[26] J. E. Hirsch *Phys. Rev. B*, vol. 28, pp. 4059–4061, 1983.

[27] G. Mazzola *et al. Phys. Rev. Lett.*, vol. 123, p. 130501, 2019.

[28] J. R. McClean *et al. Nat. Commun.*, vol. 9, no. 1, p. 4812, 2018.